ARTICLE
Journal of Cellular Biochemistry 113:946–955 (2012)

Journal of Cellular Biochemistry

Paclitaxel Inhibits Osteoclast Formation and Bone Resorption Via Influencing Mitotic Cell Cycle Arrest and RANKL-Induced Activation of NF-κB and ERK

Estabelle S. M. Ang,[1] Nathan J. Pavlos,[2] Shek Man Chim,[5] Hao Tian Feng,[2] Robin M. Scaife,[3] James H. Steer,[4] Ming H. Zheng,[2] and Jiake Xu[5*]

[1] *School of Dentistry, University of Western Australia, Nedlands, WA 6009, Australia*

[2] *Centre for Orthopaedic Research, School of Surgery, University of Western Australia, Nedlands, WA 6009, Australia*

[3] *Laboratory for Cancer Medicine, Western Australian Institute for Medical Research, University of Western Australia, Nedlands, WA 6009, Australia*

[4] *School of Medicine and Pharmacology, University of Western Australia, Nedlands, WA 6009, Australia*

[5] *School of Pathology and Laboratory Medicine, University of Western Australia, Nedlands, WA 6009, Australia*

ABSTRACT

Pathological bone destruction (osteolysis) is a hallmark of many bone diseases including tumor metastasis to bone, locally osteolytic giant cell tumor (GCT) of bone, and Paget's disease. Paclitaxel is frequently prescribed in the treatment of several malignant tumors where it has been shown to exert beneficial effects on bone lesions. However, the mechanism(s) through which paclitaxel regulates osteoclast formation and function remain ill defined. In the present study, we demonstrate that paclitaxel dose-dependently inhibits receptor activator of nuclear factor-kappa B ligand (RANKL)-induced osteoclastogenesis in both RAW264.7 cells and mouse bone marrow macrophage (BMM) systems. In addition, paclitaxel treatment reduces the bone resorptive activity of human osteoclasts derived from GCT of bone, and attenuates lipopolysaccharide (LPS)-induced osteolysis in a mouse calvarial model. Complementary cellular and biochemical analyses revealed that paclitaxel induces mitotic arrest of osteoclastic precursor cells. Furthermore, luciferase reporter gene assays and western blot analysis indicate that paclitaxel modulates key RANKL-induced activation pathways that are essential to osteoclast formation including NF-κB and ERK. Collectively, our findings demonstrate a role for paclitaxel in the regulation of osteoclast formation and function and uncover potential mechanism(s) through which paclitaxel alleviates pathological osteolysis. J. Cell. Biochem. 113: 946–955, 2012.

KEY WORDS: PACLITAXEL; OSTEOCLASTOGENESIS; BONE RESORPTION; RANKL; NF-κB

Pathological bone destruction commonly accompanies a wide range of debilitating clinical disorders including tumor metastasis to bone, primary osteolytic tumors of bone such as giant cell tumors (GCT), Paget's disease as well as inflammation-induced bone diseases including periodontitis and infection of orthopedic implants. Osteoclasts are terminally differentiated, multinucleated cells responsible for the physiological and pathological degradation of mineralized bone [Teitelbaum, 2007]. The receptor activator of nuclear factor-kappa B ligand (RANKL) is a key cytokine for osteoclast differentiation [Lacey et al., 1998]. Developing strategies that target RANKL-mediated osteoclast differentiation and bone resorption are therefore vital in the treatment of pathological osteoclast-mediated bone diseases.

Paclitaxel, which is derived from the bark of the Pacific yew tree *Taxus brevifolia*, exhibits potent efficacy against both breast and ovarian cancers [Wall and Wani, 1996; Piccart et al., 2003]. Mechanistically, paclitaxel selectively binds to tubulin and subsequently stabilizes microtubules, thus inhibiting cell division [Abal et al., 2003; Bhalla, 2003]. Interestingly, metastatic bone lesions have been reported to respond better to a combination of

Abbreviations: α-MEM, alpha-modified essential medium; BMM, bone marrow macrophage; ERK, extracellular signal-regulated kinase; JNK, c-JUN NH2-terminal protein kinase; MAPK, mitogen-activated protein kinase, osteoclast like cells; PBS, phosphate-buffered saline; NF-κB, Nuclear factor of kappa B; RANKL, the receptor activator of NF-κB ligand; TRACP, tartrate-resistant acid phosphatase.

*Correspondence to: Jiake Xu, School of Pathology and Laboratory Medicine, University of Western Australia, QEII Medical Centre, 1st Floor M Block, Nedlands WA 6009 Australia. E-mail: jiake.xu@uwa.edu.au

Received 14 October 2011; Accepted 17 October 2011 • DOI 10.1002/jcb.23423 • © 2011 Wiley Periodicals, Inc.
Published online 27 October 2011 in Wiley Online Library (wileyonlinelibrary.com).

paclitaxel and docetaxel than to a variety of single chemotherapeutic agents [Harvey, 1997]. Whilst these clinical observations point to a beneficial effect of paclitaxel on bone lesions, the underlying mechanisms of its action remain to be established.

In this study we demonstrate that paclitaxel treatment impairs osteoclast formation and function both in vitro and in vivo under pathological settings. Furthermore, we demonstrate that the inhibition in osteoclast activity by paclitaxel is due, at least in part, to a dose-dependent arrest in mitosis of pre-osteoclastic cells as well as perturbations in key pro-osteoclastogenic signaling pathways including RANKL-induced activation of NF-κB and ERK. Collectively, our data indicate that paclitaxel directly modulates osteoclast formation and function and thus may present an alternative anti-resorptive therapy for the alleviation of pathological bone destruction.

MATERIALS AND METHODS

MEDIA AND REAGENTS

RAW264.7 cells were obtained from the American Type Culture Collection (Rockville, MD). Alpha modification of eagles medium (α-MEM) and fetal bovine serum (FBS) were purchased from TRACE (Sydney, Australia). Paclitaxel was purchased from Sigma-Aldrich (Sydney, Australia) and was dissolved in ethanol. The luciferase assay system was obtained from Promega (Sydney, Australia). Annexin V-PE staining reagents was purchased from BD Biosciences Pty Ltd. (Sydney, Australia). GST-rRANKL (RANKL) was generated as previously described [Xu et al., 2000; Pavlos et al., 2005]. Macrophage-colony stimulating factor (M-CSF) was supplied by R&D (R&D Systems, Minneapolis, MN).

IN VITRO OSTEOCLASTOGENESIS ASSAY

RAW264.7 cells were seeded at a density of 1.3×10^3 cells per well in 96-well plates and cultured in the presence of α-MEM supplemented with 10% FBS, 2 mM L-glutamine and 100 U/ml penicillin/streptomycin in a humidified incubator (37°C, 5% CO_2). Cells were incubated overnight and stimulated with RANKL (100 ng/ml) in the absence or presence of paclitaxel at varying concentration. Culture media was replenished every second day. After 5-day culture, cells were fixed and stained for tartrate-resistant acid phosphatase (TRACP) activity [Xu et al., 2000]. TRACP-positive multinucleated cells (>3 nuclei) were scored as OCL cells. For primary cell culture, bone marrow macrophages (BMM) were isolated from long bones of C57BL/six mice and seeded into a 96-well plate (5×10^3 cells/well) in the presence of 50 ng/ml of M-CSF [Ang et al., 2007]. After 3 days, cells were stimulated with fresh medium containing 50 ng/ml of M-CSF and 100 ng/ml of GST-rRANKL for 7–10 days, and subjected to TRACP staining. Total number of TRACP-positive cells per well of a 96-well plate (at least three wells per group) were counted and quantified.

LIPOPOLYSACCHARIDE-INDUCED OSTEOLYSIS IN VIVO

The model for inducing osteolysis in mouse calvaria was as previously described [Li et al., 2002; Yip et al., 2004]. Injections of lipopolysaccharide (LPS) (500 μg; Sigma, Australia), LPS and paclitaxel (5 mg/kg) or phosphate buffered saline (PBS) were made into the subcutaneous tissue overlying the calvaria of 7–8 week old C57BL/six mice. Mice were sacrificed 5 days after the initial injection and the extent of bone lesions assessed by examining bone histology and TRACP activity as previously described [Li et al., 2002; Yip et al., 2004].

BONE RESORPTION PIT ASSAY

Human GCT of bone samples was freshly isolated from patients who have undergone surgery at Sir Charles Gairdner Hospital (Nedlands, Western Australia). Tumor tissues were processed as previously described [Ang et al., 2011a]. OCL cells were seeded on ~150 μm thick whale dentine slices in wells of a 96-well plate. Whale dentine was kindly donated by the decommissioned Albany Whaling Station (Albany, Western Australia). Ultra thin slices were prepared in our laboratory. The bone resorption assay was carried out as previously described [Yip et al., 2004; Yip et al., 2006]. In brief, OCL cells were incubated for 1–2 h in complete α-MEM in the presence of 5 ng/ml RANKL to allow proper attachment of cells to the bone substrate prior to the addition of paclitaxel. After additional 48 h incubation, dentine slices were fixed with 4% paraformaldehyde and stained for TRACP. The numbers of TRACP positive cells with three or more nuclei present on the dentine slices were counted under a light microscope. The dentine slices were then treated with 2 M NaOH, followed by gentle brushing and sonication to remove cells. The resorption pits created by OCL cells were visualized using a Philips XL30 scanning electron microscope and area of resorption area was calculated using the ImageJ software (NIH) and results were expressed as a percentage of total dentine area.

NF-κB REPORTER GENE ASSAYS

To examine the effects of paclitaxel on RANKL-induced NF-κB activation, RAW264.7 cells that had been stably transfected with a luciferase reporter construct, (3kB-luc-SV40) were used to determine NF-κB activation as previously described [Wang et al., 2003; Ang et al., 2011b]. Luciferase activity was measured in cell lysates using the Promega Luciferase Assay System according the manufacturer's instructions (Promega, Sydney, Australia).

APOPTOSIS ASSAY

Apoptosis assays using Annexin V-PE staining were performed as previously described [Xu et al., 2003]. In brief, RAW 264.7 cells (5×10^5) were seeded in 3 ml of complete α-MEM into wells of a six-well plate and left overnight. Cells were treated for 24 h, harvested and resuspended in 0.5 ml of 1× Annexin V Binding Buffer (BD Pharmigen, NSW, Australia). Annexin V-PE (5 μl) (BD-Pharmigen, NSW, Australia) and 7-AAD (5 μl) (BD-Pharmigen, NSW, Australia) were added to 100 μl of the cell suspension followed by gentle vortexing cells incubated for 15 min at room temperature in the dark. Four hundred microliters of 1× binding buffer was added to each tube and cells analyzed by flow cytometry (Becton Dickinson FACSCalibur) within an hour.

CONFOCAL MICROSCOPY

For immunofluorescence studies, RAW264.7 cells (1×10^4) were seeded onto 13 mm glass coverslips that were placed in 24-well plates and then stimulated with RANKL (100 ng/ml) to induce

osteoclast formation. After 5 days, osteoclast-like cells were incubated overnight in either the absence or presence of paclitaxel (100 nM). Additional experiments were carried out using human OCL cells freshly isolated from giant cell tumor of bone as previously described [Huang et al., 2000]. Following treatment, osteoclast-like cells were washed twice with 1× PBS, fixed with 4% paraformaldehyde in PBS, pH 7.4, for 15 min at room temperature and then washed extensively in PBS. Cells were then permeabilized in 0.1% Triton X-100 in PBS, washed twice in PBS containing 0.2% bovine serum albumin (BSA) and labeled with a monoclonal anti-α-tubulin antibody (Sigma, St. Louis) (1:500 diluted in 0.2% BSA-PBS) for 1 h at room temperature. Following washing (4× with 0.2% BSA-PBS, 4× with PBS, 2× with 0.2% BSA-PBS), cells were incubated with Alexa Fluor 488 secondary antibodies (Molecular Probes Inc., Eugene) at 1:500 dilution for 45 min at room temperature, or biotinylated anti-mouse (Jackson laboratories, MA) followed by Alexa Fluor 546 nm-conjugated streptavidin (Molecular Probes Inc.) diluted 1:400 in BSA-PBS. Cells were then washed in 0.2% BSA-PBS and PBS as above, counter-stained with Hoechst 33342 (Molecular Probes Inc.) (1:10,000; 3 min at room temperature), and then mounted for confocal microscopy (CLSM) (MRC-1000, Bio-Rad) as previously described [Pavlos et al., 2005; Yip et al., 2005]. To examine microfilament structure, OCL cells were stained for F-actin using Rhodamine-conjugated Phalloidin (1:200; Molecular Probes Inc.), or FITC-conjugated Phalloidin (Sigma, St. Louis), for 2 h at room temperature as previously described [Pavlos et al., 2005; Yip et al., 2005]. For microtubule staining, a monoclonal anti-α-tubulin antibody (Sigma, St. Louis) (1:500 diluted in 0.2% BSA-PBS) was used with Alexa Fluor 488 secondary antibodies (Molecular Probes Inc., Eugene) at 1:500 dilution. The fluorescent images were collected on a Bio-Rad MRC 1000/1024 UV laser scanning confocal microscopy.

CELL CYCLE ARREST

Following exposure to paclitaxel, RAW264.7 cells and OCL cells were rinsed with PBS, fixed with 4% paraformaldehyde (in PBS), permeabilized by 0.2% Triton X-100 (in PBS containing 0.5% BSA). Permeabilized cells were incubated for 60 min with anti-PH3 mouse monoclonal antibody 6G3 (Cell Signaling #9706, MA) diluted 1:2,000 into PBS with 0.5% BSA, followed by a PBS wash and incubation for 60 min with 1/400 diluted Alexa Fluor 546 nm secondary antibody (Molecular Probes, Vic, Australia) in PBS containing 0.5% BSA. Cells were imaged using a BioRad confocal microscope (40× objective lens) following staining of nuclear DNA with Hoescht 33258 (Sigma, Sydney, Australia).

WESTERN BLOT ANALYSIS

Proteins separated by SDS–PAGE were electroblotted onto Hybond-P (PVDF) membranes (Bio-Rad). Membranes were blocked with 5% (w/v) non-fat milk powder in TBST (10 mM Tris, pH7.5, 150 mM NaCl, 0.1% [v/v] Tween 20) and then probed with antibodies raised against phosphorylated ERK and α-tubulin (Cell Signaling Technology, Inc. MA) in the blocking solution. The membranes were washed three times with TBS and then incubated with appropriate Horseradish peroxidase-conjugated secondary antibodies diluted 1:5,000 in 1% (w/v) non-fat milk powder in TBST. The membranes were developed using an enhanced chemiluminescence (ECL) system (Amersham Pharmacia Biotech).

STATISTICAL ANALYSES

Results are presented as mean ± SEM from three or more experiments. Student's *t*-test was used to test statistical significance between groups. A *P*-value of <0.05 was considered to be statistically significant. All data shown represent one of at least three independent experiments.

RESULTS

PACLITAXEL INHIBITS RANKL-INDUCED OSTEOCLASTOGENESIS

To examine the effect(s) of paclitaxel on osteoclastogenesis, RAW264.7 cells were incubated with paclitaxel (10–40 nM) in the presence of RANKL. After 5 days of culture, cells were fixed and stained for TRACP activity. In the absence of paclitaxel, RAW264.7 cells differentiated into characteristic TRACP positive multinucleated OCL cells in response to RANKL. RAW264.7 cells treated with paclitaxel demonstrated a dose-dependent inhibition of RANKL-induced formation of OCL cells (Fig. 1A,B). To determine whether the observed decrease in osteoclast formation was due to cell apoptosis, RAW264.7 cells were treated with paclitaxel (10–100 nM) for 24 h and subjected to Annexin V staining and FACS analysis. As shown in Figure 1C, whereas Paclitaxel failed to induce apoptosis at concentrations of 10–20 nM that were deemed effective in inhibiting osteoclastogenesis, at higher doses i.e., 50 and 100 nM, paclitaxel markedly induced cell apoptosis (18 and 55%, respectively) (Fig. 1C).

To further validate the inhibitory effects of paclitaxel on osteoclastogenesis, we also examined its effect on a mouse primary BMM osteoclastogenic culture system. To this end, paclitaxel (2.5, 5, 10, and 20 nM) was added to BMM progenitor cultures. After 7 days, cells were fixed, stained for TRACP activity and formation of OCL cells quantitated. Consistent with its effect on RAW264.7 cells, paclitaxel dose-dependently inhibited osteoclast formation from BMM-derived cells (Fig. 2A,B).

PACLITAXEL INHIBITS BONE RESORPTION BY OCL CELLS DERIVED FROM GCT OF BONE

To examine the effect of paclitaxel on osteoclastic bone resorption, human osteoclasts, freshly derived from GCT of bone, were seeded onto dentine slices and cultured in the presence of vehicle or a sublethal dose of paclitaxel (20 nM) for 48 h. Representative images of TRACP positive OCL cells on dentine slice and resorption pits taken by light and scanning electron microscopy are illustrated in Figure 3A. Paclitaxel (20 nM) inhibited bone resorption ($P < 0.001$) (Fig. 3B) without affecting the total number of OCL cells per dentine slice (Fig. 3C). In the paclitaxel-treated group, there were many single pits, whereas multiple pits are seen in the control dentine slice. These results indicate that paclitaxel is capable of suppressing bone resorption by OCL cells derived from GCT.

PACLITAXEL INHIBITS LPS-INDUCED OSTEOLYSIS IN THE MOUSE CALVARIUM MODEL

Next, we sought to determine the effects of paclitaxel on pathological osteolysis in vivo. To this end, we employed a well-characterized model of LPS-induced osteolysis in the mouse

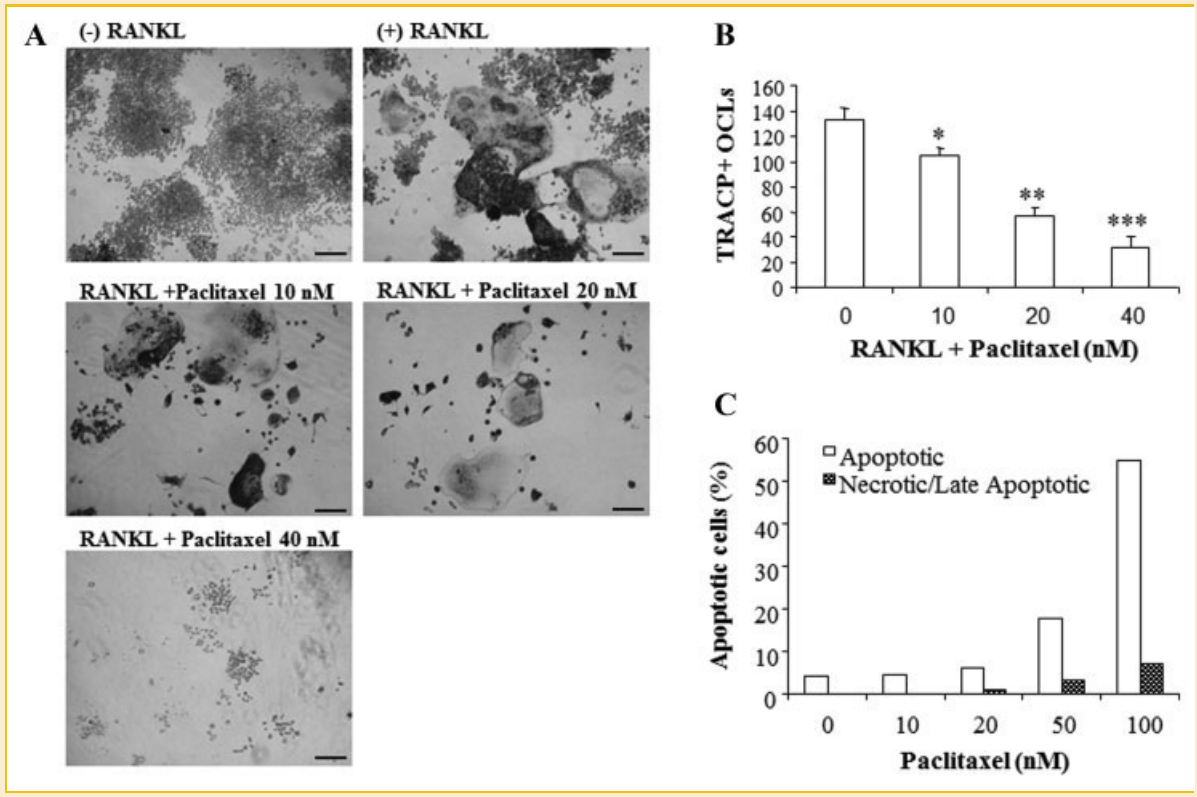

Fig. 1. A–B: Paclitaxel inhibits RANKL-induced RAW264.7 cell differentiation into OCL cells. RAW264.7 cells were cultured in a 96-well plate in the presence of 100 ng/ml RANKL for 5 days in the presence or absence of paclitaxel. A: After 5 days, the cells were fixed with 4% paraformaldehyde and stained for TRACP activity. Representative images of triplicate wells from one of three experiments are shown. Bars, 30 μm. B: TRACP positive multinucleated cells with more than three nuclei were counted. (mean ± SD from triplicate wells; $^{*}P < 0.05$, $^{**}P < 0.01$, $^{***}P < 0.001$, compared to untreated controls). C: Paclitaxel dose dependently increases apoptosis and necrosis in RAW264.7 cells. The percentage of AnnexinV-PE (apoptotic) and 7-AAD (necrotic/late apoptotic) positive RAW264.7 cells, following 24 h exposure to paclitaxel (1–100 nM), was determined by flow cytometry (10,000 cells were counted at each point).

calvarium [Li et al., 2002; Yip et al., 2004]. As expected, LPS treatment enhanced the eroded surface of bone 5 days after injection as compared to PBS injection (Fig. 4A). Closer examination revealed that there was an abundance of TRACP positive OCL cells present on the surface of the eroded bone in LPS-injected mice (Fig. 4B,C). By comparison, paclitaxel significantly reduced the area of osteolytic cavities within LPS treated calvaria (Fig. 4A). In addition, the total TRACP staining was reduced (Fig. 4B,C) indicating that paclitaxel reduced LPS-induced formation of OCLs. Together, these results demonstrate the propensity of paclitaxel to inhibit osteolysis in vivo.

EFFECT OF PACLITAXEL ON THE CYTOSKELETAL ORGANIZATION OF OCL CELLS

To explore the underlying mechanisms by which paclitaxel inhibits osteoclast function, we first examined its effects on the cytoskeletal organization of RAW264.7 cell-derived OCL cells. For this purpose, RAW264.7 cells were seeded onto glass coverslips in a 24-well cell culture plate and stimulated with RANKL to generate OCL cells. After 5-days culture, OCL cells were treated with paclitaxel (10, 50, and 100 nM) for 16 h. OCL cells were then fixed and immunostained with Rhodamine-conjugated Phalloidin and Hoechst 33342 to visualize cytoskeletal (F-actin) and nuclear morphology, respectively. As shown in Figure 5A, untreated OCL (vehicle) cells displayed a pronounced and contiguous F-actin rich podosomal belt (red) and intact nuclei (blue) (Fig. 5A). By comparison, OCL cells treated with paclitaxel displayed striking morphological aberrations. At doses (50 and 100 nM) of paclitaxel, OCL cells displayed disorganization of podosomes and F-actin filaments and some nuclear fragmentation, indicative of cellular apoptosis (Fig. 5A). On the other hand, only very subtle changes in the F-actin/podosomal integrity were observed in OCL cells at dose of 10 nM.

Similar morphological disturbances were observed in OCL cells derived from mouse BMM and human GCT. In this instance, OCL cells were treated overnight with varying concentrations of paclitaxel (10–100 nM). OCL cells were subsequently fixed and triple-stained with Rhodamine-conjugated Phalloidin, α-tubulin, and Hoechst 33342 to visualize microfilaments, microtubules, and chromatin, respectively. As shown in Figure 5B, untreated BMM-derived OCL cells displayed characteristic podosomal belts (red), a spatially organized microtubule array (green) and intact nuclei (blue), whereas OCL cells treated with paclitaxel at doses >50 nM exhibited changes in the integrity of F-actin and microtubule organization, and nuclear fragmentation (Fig. 5B). Microtubule clustering and bundling was also observed in some cells (Fig. 5B, green staining), consistent with the reported role of paclitaxel as a microtubule stabilizer. Similar effects were also observed in GCT-derived OCL cells (Fig. 5C). Overall, these results

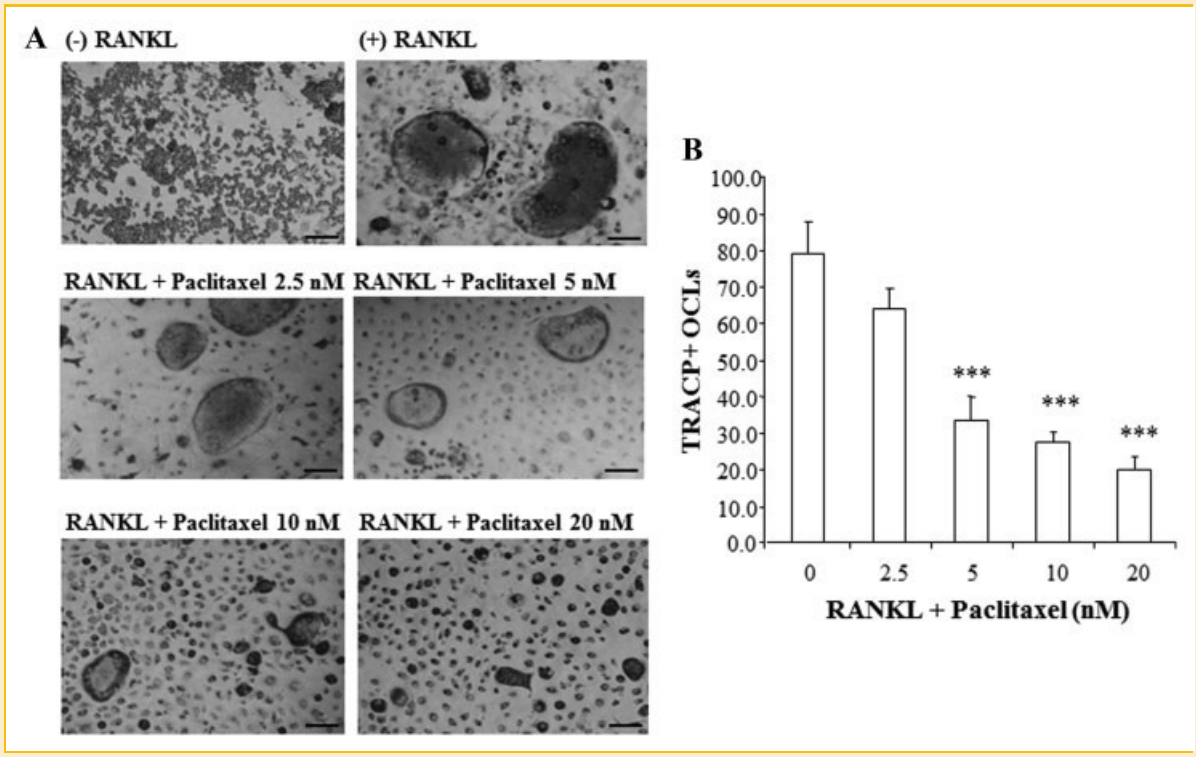

Fig. 2. Paclitaxel inhibits RANKL-induced osteoclastogenesis in primary cell cultures. Freshly isolated BMM from C57BL/six mice were cultured in a 96-well plate in the presence of M-CSF for the first 3 days and then M-CSF and 100 ng/ml of RANKL for an additional 7 days with or without paclitaxel. A: After 10 days, cells were fixed with 4% paraformaldehyde and stained for TRACP activity. Representative images of triplicate wells from one of three experiments are shown. Bars, 20 μm. B: Quantitation of the effect of paclitaxel on RANKL-induced osteoclastogenesis. TRACP positive OCL cells (>10 nuclei) are scored (***P value <0.001, compared to untreated control).

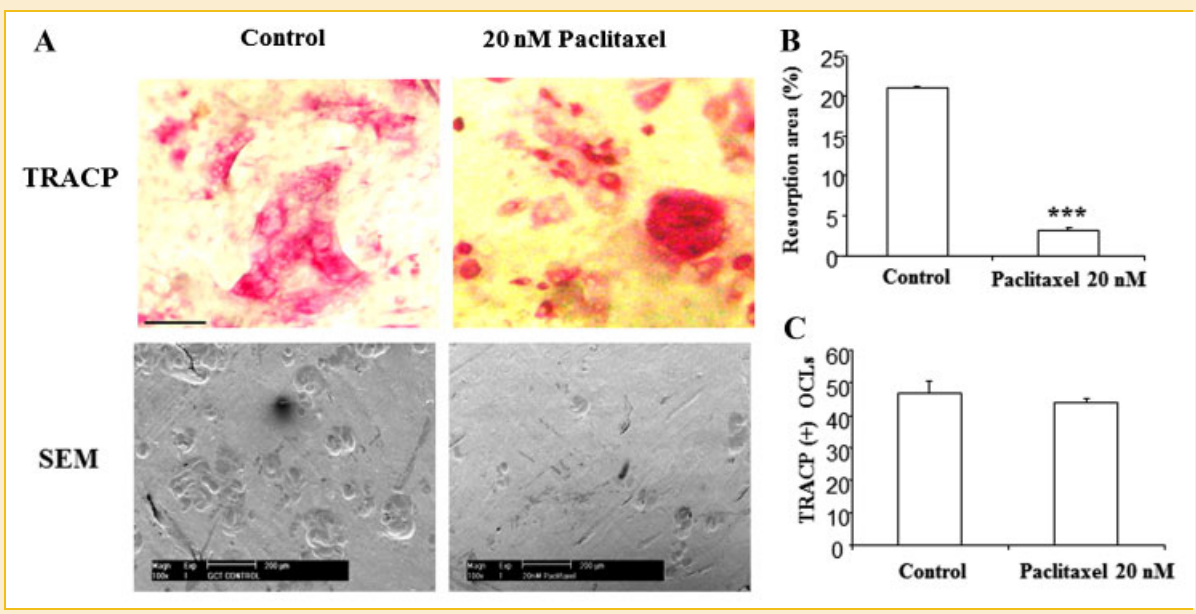

Fig. 3. Paclitaxel inhibits the bone resorptive activity of the multinucleated giant cells that were isolated from patients presenting with giant cell tumor of bone. Cells were seeded on dentine slice in the presence of paclitaxel (20 nM). A: After 48 h, dentine slices were fixed with 4% paraformaldehyde and stained for TRACP activity (top panel) and analyzed using scanning electron microscopy (bottom panel). Representative images of triplicate wells from one of three experiments are shown. Bars, 20 μm. B: Quantitation of the effect of paclitaxel on bone resorption. Percentage of resorption area was measured (mean + SD) (***P value <0.001). C: Total OCL cell numbers per dentine slice (mean + SD) (***P value <0.001).

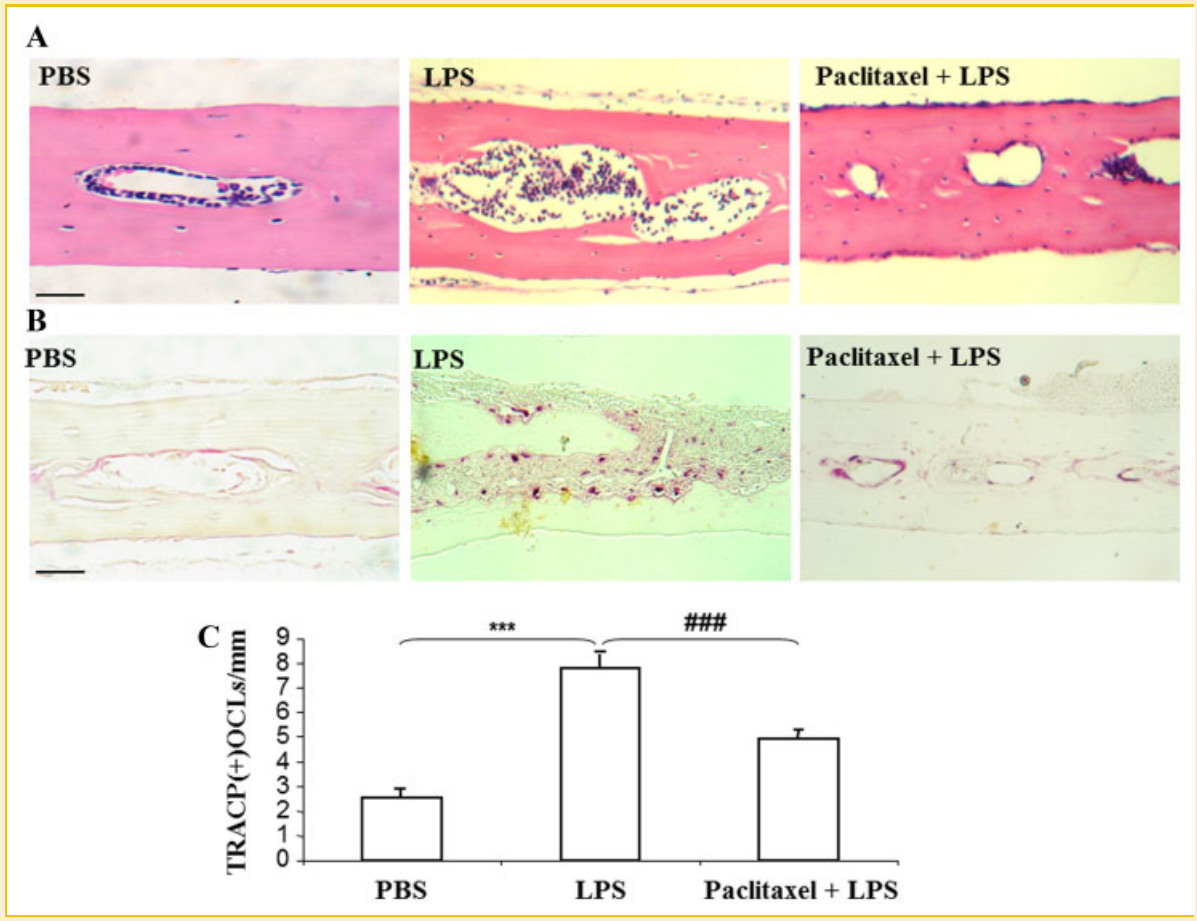

Fig. 4. Paclitaxel inhibits LPS-induced osteolysis in vivo. LPS (500 μg) was injected locally into the subcutaneous tissue overlying calvaria of C57BL/six mice in the presence or absence of paclitaxel (5 mg/kg). PBS served as a control. After 5 days, bone destruction and osteoclast activity was assessed by (A) histology (H&E stain) and (B) TRACP stain. Representative images from three replicates are shown. Bars, 50 μm. C: Osteoclast density (osteoclasts/mm) was determined (mean + SD; $^{***}P < 0.001$ compared to PBS control, $###P < 0.001$ compared to LPS control).

indicate that while paclitaxel treatment at doses that inhibited osteoclastogenesis did not have an obvious impact on cytoskeletal organization, paclitaxel induces pronounced cytoskeletal aberrations at higher doses consistent with the morphological onset of apoptosis.

PACLITAXEL CAUSES G2/M CELL CYCLE ARREST IN RAW264.7 CELLS AND OCL CELLS

By blocking microtubule dynamics, paclitaxel has been shown to cause mitotic arrest in pro-metaphase, followed by mitotic catastrophe and apoptosis [Jordan and Wilson, 2004]. We therefore examined mitotic arrest in paclitaxel treated RAW264.7 cells and OCL cells. Progression of the cells to mitosis was monitored by fluorescence microscopy following staining with the mitosis-specific anti-phospho-histone 3 marker [Scaife, 2005]. We found that RAW264.7 cells rapidly accumulate in pro-metaphase in the presence of paclitaxel (Fig. 6A). Furthermore, paclitaxel induced dose-dependent accumulation of mitotic arrested cells is paralleled by its effect on apoptosis (Fig. 6B). Interestingly, following RANKL-induced differentiation, paclitaxel resulted in an intermediate stage of OCL cell differentiation represented by large hyperploid RAW264.7 cells mitotically arrested (Fig. 6C, Arrow). Furthermore, prolonged exposure to paclitaxel led to mitotic catastrophe-associated micronucleation in both precursor RAW264.7 cells and OCL cells (Fig. 6D, Arrow).

PACLITAXEL INHIBITS RANKL-INDUCED ACTIVATION OF NF-κB AND ERK SIGNALLING

To examine the effect of paclitaxel on RANKL-induced NF-κB activation, RAW264.7 cells stably transfected with a NF-κB driven luciferase reporter construct were stimulated with RANKL (100 ng/ml) for 8 h with or without 1 h of pretreated with paclitaxel (1, 10, or 50 nM). As shown in Figure 7A, RANKL induced NF-κB activity was dose dependently inhibited by paclitaxel.

Next, the effect of paclitaxel on RANKL-induced ERK phosphorylation was examined. Western blot analysis demonstrated increased phosphorylation of ERK 15 and 30 min after RANKL stimulation. Pretreatment with paclitaxel (10 nM) slightly decreased RANKL-induced ERK phosphorylation (at both 15 and 30 min, Figure 7B).

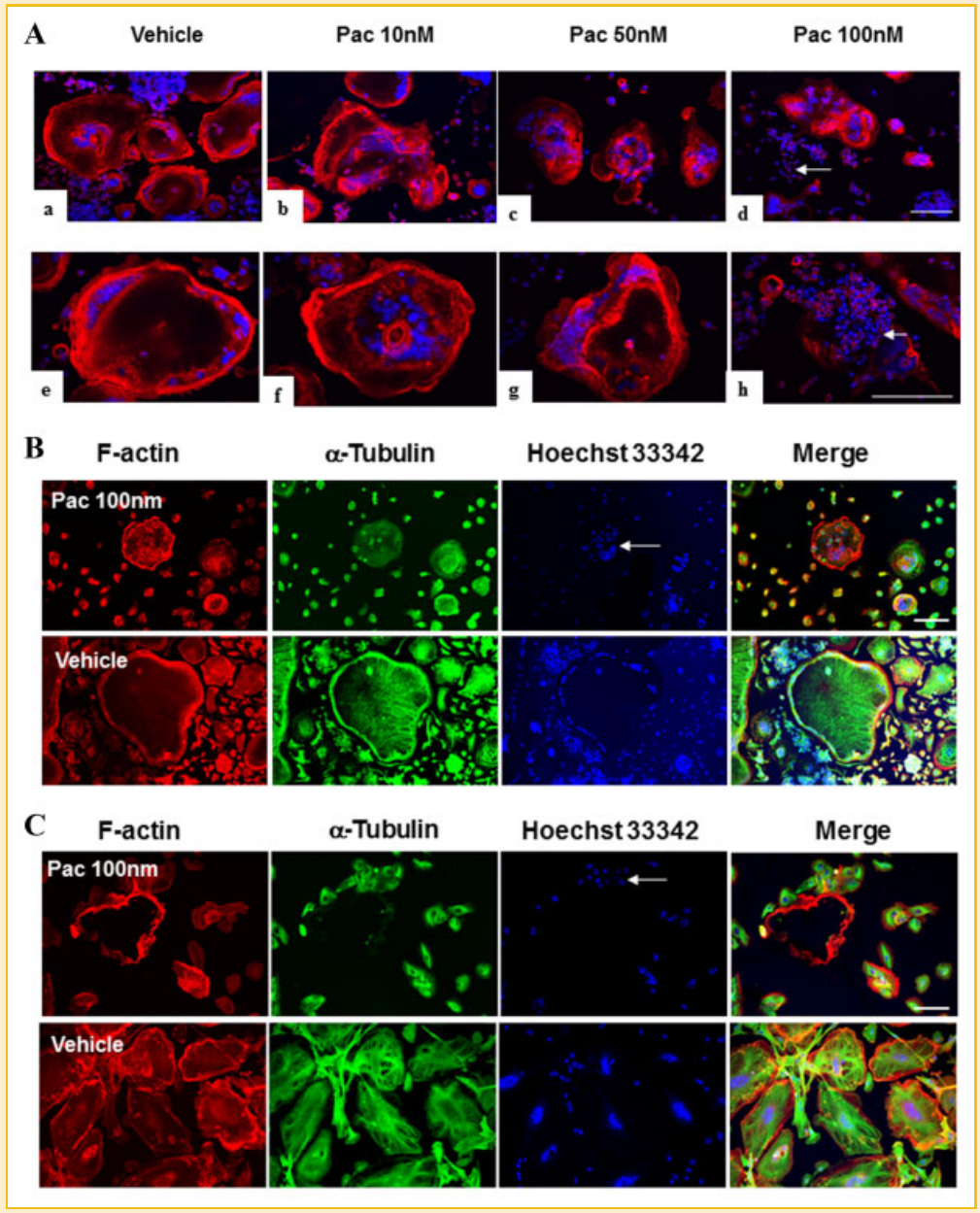

Fig. 5. The effect of paclitaxel on cytoskeletal organization in OCL cells. A: RAW264.7 cell derived OCL cells were treated with 10, 50, and 100 nM paclitaxel or left untreated overnight (24 h) and fixed with 4% paraformaldehyde and stained with Hoechst 33342 dye and F-actin antibody. a–d: Confocal images at low magnification ×20; e–h: Confocal images at high magnification ×40 showing the nuclei staining (blue) and F-actin structure (red) in the paclitaxel treated cells. B: The effect of paclitaxel on BMM derived OCL cells. Confocal images are shown for the F-actin (red), α-tubulin (green), and nuclei staining (blue) in the paclitaxel (100 nM) treated or control cells. C: The effect of paclitaxel on human GCT-derived OCL cells. Confocal images were shown for the F-actin (red), α-tubulin (green), and nuclei staining (blue). Arrows indicate the presence of nuclear fragmentation. Bars, 20 μm.

DISCUSSION

Pathological bone destruction occurs when osteoclasts are over-active and present in elevated numbers, leading to excessive breakdown of bone. In this study, we document the effect of paclitaxel on inhibition of osteoclast formation and induction of osteoclast apoptosis, substantiating previous findings that paclitaxel inhibits osteoclast bone resorption [Hall et al., 1995]. In addition, we have shown that paclitaxel inhibits LPS-induced osteolysis in vivo and inhibits the bone resorptive activity of multinucleated giant cells derived from patients presenting with GCT. Paclitaxel has been widely used therapeutically for the treatment of several malignant tumors, thus our findings provide a possible mechanistic explanation for its beneficial effect on bone lesions observed in clinical settings [Harvey, 1997]. Whilst, in vitro, paclitaxel has been used to trigger cancer cell death at doses ranging from 10 to 1,000 nM [Ray et al., 1994], we found that paclitaxel effectively inhibits osteoclastogenesis at doses range of 5–20 nM.

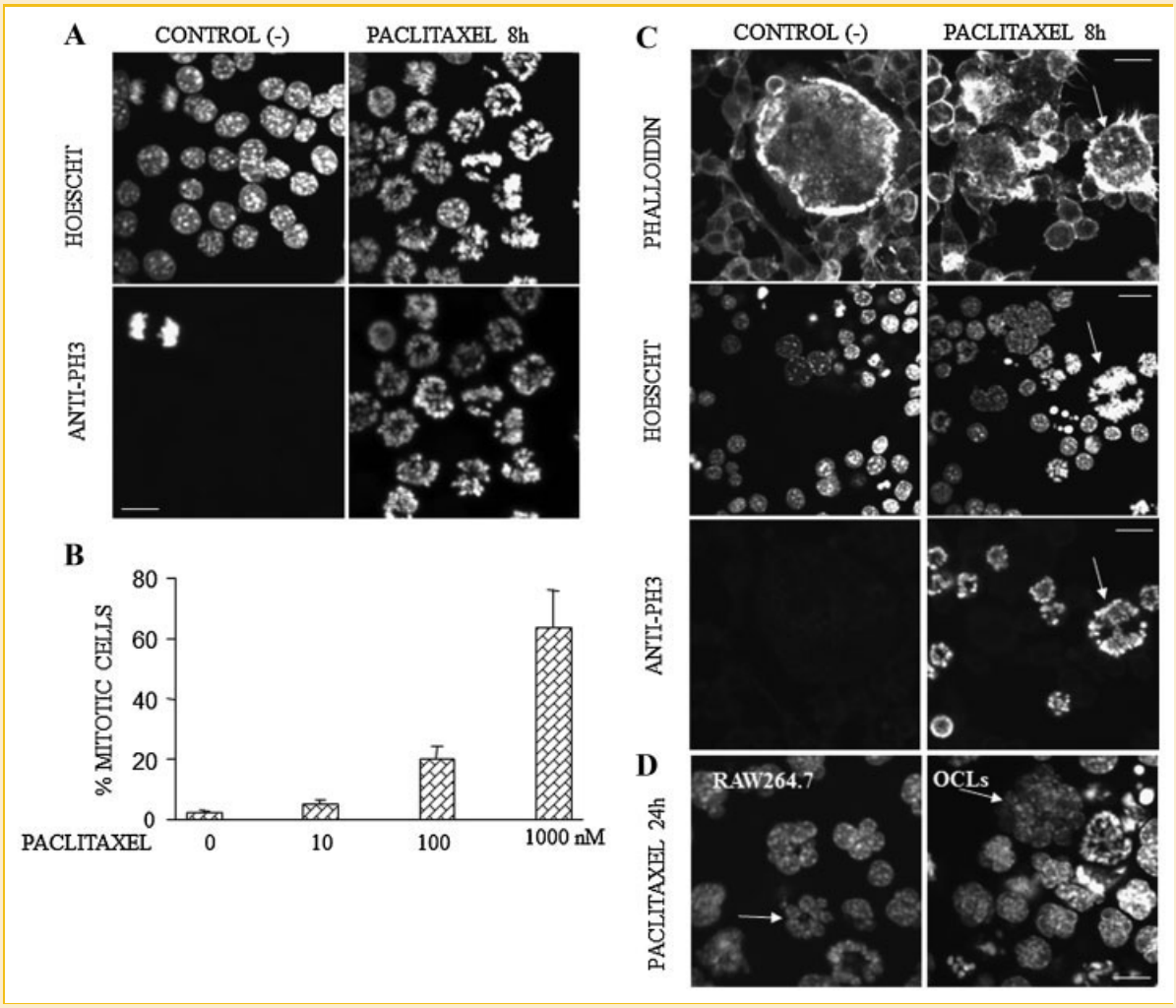

Fig. 6. Paclitaxel leads to cell cycle arrest in G2/M and mitotic catastrophe in RAW264.7 cells and OCL cells. A: RAW264.7 cells were either left untreated or exposed to 1 μM paclitaxel for 8 h and then fixed and stained with Hoescht 33258 and anti-phospho-histone H3. B: The percentage of RAW264.7 cells that stained with anti-phospho-histone H3 following an 8 h exposure to 0, 10, 100, and 1,000 nM paclitaxel. C: RAW264.7 cells were treated with 100 ng/ml of RANKL for 4 days, followed by further 24 h incubation with or without 1 μM paclitaxel. The cells were then fixed and stained with Hoescht 33258, FITC-phalloidin and anti-phospho-histone H3. D: RAW264.7 cells were either left untreated (left panel) or exposed to RANKL for 4 days (right panel) and then treated with 1 μM paclitaxel for 24 h before being fixed and stained with Hoescht 33258 dye. White arrows indicate micronucleation. Bars, 10 μm.

Previous studies have shown that paclitaxel binds to β-tubulin and inhibits microtubule dynamic instability, leading to apoptosis in several cell types [Abal et al., 2003; Bhalla, 2003]. Inhibition of microtubule dynamics causes mitotic arrest, and this is followed by micronucleation and apoptosis [Bacus et al., 2001]. Our finding that paclitaxel causes G2/M arrest and micronucleation of OCL cells, indicates that the inhibitory effect of paclitaxel on osteoclast formation is also due to targeting progression of the cell cycle that results in mitotic arrest followed by mitotic catastrophe-associated apoptosis of precursor cells and intermediately differentiated stages of OCL cells.

RANKL-induced NF-κB signaling pathways are important in osteoclastogenesis and survival [Xing et al., 2002; Xu et al., 2009]. It has been reported that paclitaxel transiently increases NF-κB activity, followed by a decrease in NF-κB activity [Mabuchi et al., 2004]. This mimics some aspects of the actions of endotoxic bacterial LPS on NF-κB activity in murine macrophages [Hwang and Ding, 1995]. Paclitaxel has also been reported to induce the phosphorylation and degradation of IkappaB-alpha, and activation of NF-κB in paclitaxel-sensitive tumor cell lines such as human breast cancer BCap37 and human epidermoid carcinoma KB cells [Dziadyk et al., 2004]. It appears that the paclitaxel-induced activation of NF-κB is dose-dependent and requires a concentration not less than 5 μM paclitaxel [Perera et al., 1996]. By comparison, our osteoclast culture model studies have used much lower paclitaxel concentrations (10–50 nM) producing an inhibition of NF-κB activity. This suggests that the action of paclitaxel on NF-κB is both dose- and cell type-dependent.

The ERK kinase signaling pathway has also been implicated in osteoclast differentiation and survival [Hotokezaka et al., 2002; Nakamura et al., 2003]. Paclitaxel has been shown to cause activation of c-JUN NH2-terminal protein kinase (JNK), concomitant

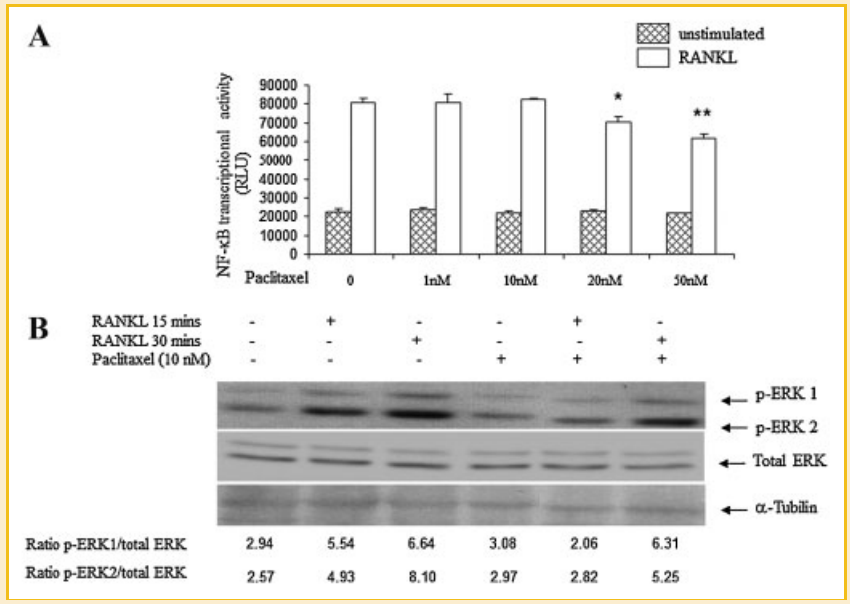

Fig. 7. Paclitaxel reduces RANKL stimulated NF-κB and ERK signaling. A: RAW264.7 cells, stably transfected with a NF-κB transcriptional luciferase reporter construct, were pretreated with paclitaxel (10 nM) for 2 h and then exposed to RANKL (100 ng/ml) or medium alone for 8 h. Results are expressed as means + SD of triplicate relative light units ($^{*}P < 0.05$, $^{**}P < 0.01$ compared to RANKL alone treated control). B: RAW264.7 cells were pretreated with vehicle alone (mock) or paclitaxel (10 nM) for 2 h followed by 100 ng/ml of RANKL for 0, 15, and 30 min. Whole cell extracts were analyzed for phosphorylated forms of ERK by western blot analysis. Membranes were probed sequentially with antibodies to p-ERK, total-ERK, and α-tubulin. Bands were detected using ECL and quantitated by densitometry. Results from a representative of triplicate experiments are shown. The levels of p-ERK1/2 proteins are shown as a ratio to total-ERK1/2.

with an inactivation of ERK [Stone and Chambers, 2000]. In this study, we found that pretreatment with paclitaxel decreases RANKL-induced ERK activation, which is consistent with the inhibitory effect of paclitaxel on osteoclast formation and function. The extent and kinetics of RANKL signaling pathways influenced by paclitaxel may contribute to the overall effects on osteoclast differentiation and activity.

In summary, this study demonstrates that paclitaxel has an inhibitory effect on osteoclastogenesis and bone resorption in vitro and in vivo. The inhibitory effects of this naturally occurring compound on OCL cells are accompanied by mitotic cell cycle arrest and the modulation of RANKL-induced NF-κB and ERK signaling pathways. Our studies suggest that paclitaxel might offer a favorable therapeutic profile for the inhibition of osteolysis.

ACKNOWLEDGMENTS

This work was supported in part by the National Health and Medical Research Council of Australia, Arthritis Foundation of Western Australia and Small Research Grant by The University of Western Australia. Estabelle Ang was a recipient of a National Health and Medical research Council of Australia (NHMRC)/Osteoporosis Australia Scholarship. Nathan J. Pavlos is supported by an NHMRC (C. J. Martin) Overseas Biomedical Fellowship ID: 463911.

REFERENCES

Abal M, Andreu JM, Barasoain I. 2003. Taxanes: Microtubule and centrosome targets, and cell cycle dependent mechanisms of action. Curr Cancer Drug Targets 3:193–203.

Ang E, Liu Q, Qi M, Liu HG, Yang X, Chen H, Zheng MH, Xu J. 2011a. Mangiferin attenuates osteoclastogenesis, bone resorption, and RANKL-induced activation of NF-kappaB and ERK. J Cell Biochem 112:89–97.

Ang ES, Yang X, Chen H, Liu Q, Zheng MH, Xu J. 2011b. Naringin abrogates osteoclastogenesis and bone resorption via the inhibition of RANKL-induced NF-kappaB and ERK activation. FEBS Lett 585:2755–2762.

Ang ES, Zhang P, Steer JH, Tan JW, Yip K, Zheng MH, Joyce DA, Xu J. 2007. Calcium/calmodulin-dependent kinase activity is required for efficient induction of osteoclast differentiation and bone resorption by receptor activator of nuclear factor kappa B ligand (RANKL). J Cell Physiol 212: 787–795.

Bacus SS, Gudkov AV, Lowe M, Lyass L, Yung Y, Komarov AP, Keyomarsi K, Yarden Y, Seger R. 2001. Taxol-induced apoptosis depends on MAP kinase pathways (ERK and p38) and is independent of p53. Oncogene 20:147–155.

Bhalla KN. 2003. Microtubule-targeted anticancer agents and apoptosis. Oncogene 22:9075–9086.

Dziadyk JM, Sui M, Zhu X, Fan W. 2004. Paclitaxel-induced apoptosis may occur without a prior G2/M-phase arrest. Anticancer Res 24:27–36.

Hall TJ, Jeker H, Schaueblin M. 1995. Taxol inhibits osteoclastic bone resorption. Calcif Tissue Int 57:463–465.

Harvey HA. 1997. Issues concerning the role of chemotherapy and hormonal therapy of bone metastases from breast carcinoma. Cancer 80:1646–1651.

Hotokezaka H, Sakai E, Kanaoka K, Saito K, Matsuo K, Kitaura H, Yoshida N, Nakayama K. 2002. U0126 and PD98059, specific inhibitors of MEK, accelerate differentiation of RAW264.7cells into osteoclast-like cells. J Biol Chem 277:47366–47372.

Huang L, Xu J, Wood DJ, Zheng MH. 2000. Gene expression of osteoprotegerin ligand, osteoprotegerin, and receptor activator of NF-kappaB in giant cell tumor of bone: Possible involvement in tumor cell-induced osteoclast-like cell formation. Am J Pathol 156:761–767.

Hwang S, Ding A. 1995. Activation of NF-kappa B in murine macrophages by taxol. Cancer Biochem Biophys 14:265–272.

Jordan MA, Wilson L. 2004. Microtubules as a target for anticancer drugs. Nat Rev Cancer 4:253–265.

Lacey DL, Timms E, Tan HL, Kelley MJ, Dunstan CR, Burgess T, Elliott R, Colombero A, Elliott G, Scully S, Hsu H, Sullivan J, Hawkins N, Davy E, Capparelli C, Eli A, Qian YX, Kaufman S, Sarosi I, Shalhoub V, Senaldi G, Guo J, Delaney J, Boyle WJ. 1998. Osteoprotegerin ligand is a cytokine that regulates osteoclast differentiation and activation. Cell 93:165–176.

Li L, Khansari A, Shapira L, Graves DT, Amar S. 2002. Contribution of interleukin-11 and prostaglandin(s) in lipopolysaccharide-induced bone resorption in vivo. Infect Immun 70:3915–3922.

Mabuchi S, Ohmichi M, Nishio Y, Hayasaka T, Kimura A, Ohta T, Kawagoe J, Takahashi K, Yada-Hashimoto N, Seino-Noda H, Sakata M, Motoyama T, Kurachi H, Testa JR, Tasaka K, Murata Y. 2004. Inhibition of inhibitor of nuclear factor-kappaB phosphorylation increases the efficacy of paclitaxel in in vitro and in vivo ovarian cancer models. Clin Cancer Res 10:7645–7654.

Nakamura H, Hirata A, Tsuji T, Yamamoto T. 2003. Role of osteoclast extracellular signal-regulated kinase (ERK) in cell survival and maintenance of cell polarity. J Bone Miner Res 18:1198–1205.

Pavlos NJ, Xu J, Riedel D, Yeoh JS, Teitelbaum SL, Papadimitriou JM, Jahn R, Ross FP, Zheng MH. 2005. Rab3D regulates a novel vesicular trafficking pathway that is required for osteoclastic bone resorption. Mol Cell Biol 25:5253–5269.

Perera PY, Qureshi N, Vogel SN. 1996. Paclitaxel (Taxol)-induced NF-kappaB translocation in murine macrophages. Infect Immun 64:878–884.

Piccart MJ, Bertelsen K, Stuart G, Cassidy J, Mangioni C, Simonsen E, James K, Kaye S, Vergote I, Blom R, Grimshaw R, Atkinson R, Swenerton K, Trope C, Nardi M, Kaern J, Tumolo S, Timmers P, Roy JA, Lhoas F, Lidvall B, Bacon M, Birt A, Andersen J, Zee B, Paul J, Pecorelli S, Baron B, McGuire W. 2003. Long-term follow-up confirms a survival advantage of the paclitaxel-cisplatin regimen over the cyclophosphamide-cisplatin combination in advanced ovarian cancer. Int J Gynecol Cancer 13(Suppl 2): 144–148.

Ray S, Ponnathpur V, Huang Y, Tang C, Mahoney ME, Ibrado AM, Bullock G, Bhalla K. 1994. 1-beta-D-arabinofuranosylcytosine-, mitoxantrone-, and paclitaxel-induced apoptosis in HL-60cells: Improved method for detection of internucleosomal DNA fragmentation. Cancer Chemother Pharmacol 34:365–371.

Scaife RM. 2005. Selective and irreversible cell cycle inhibition by diphenyleneiodonium. Mol Cancer Ther 4:876–884.

Stone AA, Chambers TC. 2000. Microtubule inhibitors elicit differential effects on MAP kinase (JNK, ERK, and p38) signaling pathways in human KB-3 carcinoma cells. Exp Cell Res 254:110–119.

Teitelbaum SL. 2007. Osteoclasts: What do they do and how do they do it? Am J Pathol 170:427–435.

Wall ME, Wani MC. 1996. Camptothecin and taxol: From discovery to clinic. J Ethnopharmacol 51:239–253 discussion 253–4.

Wang C, Steer JH, Joyce DA, Yip KH, Zheng MH, Xu J. 2003. 12-O-tetradecanoylphorbol-13-acetate (TPA) inhibits osteoclastogenesis by suppressing RANKL-induced NF-kappaB activation. J Bone Miner Res 18: 2159–2168.

Xing L, Bushnell TP, Carlson L, Tai Z, Tondravi M, Siebenlist U, Young F, Boyce BF. 2002. NF-kappaB p50 and p52 expression is not required for RANK-expressing osteoclast progenitor formation but is essential for RANK- and cytokine-mediated osteoclastogenesis. J Bone Miner Res 17:1200–1210.

Xu J, Feng HT, Wang C, Yip KH, Pavlos N, Papadimitriou JM, Wood D, Zheng MH. 2003. Effects of Bafilomycin A1: An inhibitor of vacuolar H (+)-ATPases on endocytosis and apoptosis in RAW cells and RAW cell-derived osteoclasts. J Cell Biochem 88:1256–1264.

Xu J, Tan JW, Huang L, Gao XH, Laird R, Liu D, Wysocki S, Zheng MH. 2000. Cloning, sequencing, and functional characterization of the rat homologue of receptor activator of NF-kappaB ligand. J Bone Miner Res 15:2178–2186.

Xu J, Wu HF, Ang ES, Yip K, Woloszyn M, Zheng MH, Tan RX. 2009. NF-kappaB modulators in osteolytic bone diseases. Cytokine Growth Factor Rev 20:7–17.

Yip KH, Feng H, Pavlos NJ, Zheng MH, Xu J. 2006. p62 ubiquitin binding-associated domain mediated the receptor activator of nuclear factor-kappaB ligand-induced osteoclast formation: A new insight into the pathogenesis of Paget's disease of bone. Am J Pathol 169:503–514.

Yip KH, Zheng MH, Feng HT, Steer JH, Joyce DA, Xu J. 2004. Sesquiterpene lactone parthenolide blocks lipopolysaccharide-induced osteolysis through the suppression of NF-kappaB activity. J Bone Miner Res 19:1905–1916.

Yip KH, Zheng MH, Steer JH, Giardina TM, Han R, Lo SZ, Bakker AJ, Cassady AI, Joyce DA, Xu J. 2005. Thapsigargin modulates osteoclastogenesis through the regulation of RANKL-induced signaling pathways and reactive oxygen species production. J Bone Miner Res 20:1462–1471.